Supporting Information

Dechlorination of Excess Trichloroethene by Bimetallic and Sulfidated Nanoscale Zero-Valent Iron

Feng He[1, 2*], *Zhenjie Li*[1], *Shasha Shi*[1], *Wenqiang Xu*[1], *Hanzhen Sheng*[1], *Yawei Gu*[1], *Yonghai Jiang*[3, 4], *Beidou Xi*[3, 4]

[1]College of Environment, Zhejiang University of Technology, Hangzhou 310014, China

[2]Key Laboratory of Microbial Technology for Industrial Pollution Control of Zhejiang Province, Zhejiang University of Technology, Hangzhou 310014, China

[3]State Key Laboratory of Environmental Criteria and Risk Assessment, Chinese Research Academy of Environmental Sciences, Beijing 100012, China

[4]State Environmental Protection Key Laboratory of Simulation and Control of Groundwater Pollution, Chinese Research Academy of Environmental Sciences, Beijing 100012, China

*Corresponding author: Feng He

Email: fenghe@zjut.edu.cn, Phone: 86-571-88871509

Number of pages: 28

Number of figures: 15

Number of tables: 6

06/28/2018

Materials and Methods

Chemicals. Ferrous sulfate ($FeSO_4$•$7H_2O$) (99.0+%, AR), and nickle sulfate hexahydrate ($NiSO_4 \cdot 6H_2O$) (98.5+%, AR) were purchased form Sinopharm Chemical Reagent Co., Ltd (Shanghai, China). Copper(II) sulfate pentahydrate ($CuSO_4$•$5H_2O$) (99+%) was purchased from Shanghai Zhenxin Reagent Co., Ltd (Shanghai, China). Sodium borohydride ($NaBH_4$) (98%), potassium tetrachloropalladate (K_2PdCl_4) (99.95%), silver nitrate ($AgNO_3$) (99.8%, AR), sodium sulfide nonahydrate (Na_2S•$9H_2O$) (98+%, AR), and concentrated HCl (37%) were purchased from Aladdin (Shanghai, China). TCE (99%, GC grade), methanol (>99%, GC), and liquid chlorinated ethene standards in methanol including TCE (1000 ppm), cis-DCE (1000 ppm), trans-DCE (1000 ppm), 1,1-DCE (1000 ppm), and VC (1000 ppm) were also supplied by Aladdin. Gaseous alkane, alkene and alkyne standards (1000 ppm of methane, ethene, ethane, acetylene, propene, propane, butene, butane, pentene, pentane, hexene and hexane) were provided by Dalian Special Gases Co., Ltd (Dalian, China). Ultrahigh purity nitrogen, hydrogen and air were supplied by Hangzhou Special Gas Co., Ltd (Hangzhou, China) for GC measurements.

Particle Preparation. All solutions were deoxygenated before use by bubbling nitrogen gas for at least 30 mins. The nZVI particles were synthesized by borohydride method adapted from Liu et al.[1] Briefly, 20 g $FeSO_4$•$7H_2O$ was dissolved into 1L 30% (volume) methanol/deionized water solution under continuous mixing, followed by addition of 50 mL $NaBH_4$ aqueous solution (2.1 M)

dropwisely using a syringe pump at a rate of ~ 0.5 mL/s. The resulting particle suspension was centrifuged, alternately washed with methanol and water for three times, and then dried under argon and stored in an anaerobic glove chamber.

The CMC-Pd nanoparticles were synthesized by reducing Pd^{2+} ions in a CMC aqueous solution using sodium borohydride ($NaBH_4$). Specifically, a 1 mL aliquot of a 0.05M $K_2PdCl_4 \cdot 3H_2O$ aqueous solution was added to 250 mL of a CMC aqueous solution (0.15 wt%). Then, a 0.05 M $NaBH_4$ aqueous solution (around 3.5 mL) was added to the mixture under constant stirring at room temperature (~23 °C). After stirring for 24 hours, the resultant CMC-Pd nanoparticles were used for catalytic hydrodechlorination of TCE in the presence of H_2 at varied headspace concentrations.

Reaction Systems. Batch experiments were conducted in 64 mL glass vials sealed with PTFE septa lined caps. The reactors were prepared in an argon-filled glove-box and contained 32 mL of deoxygenated HEPES buffer solution (25 mM, pH = 8), 32 mL of headspace, and specified quantities of nZVIs and TCE. The desired starting concentration of TCE (94 μM and 2.8 mM) was obtained by injecting either 18 μL 0.136 M or 54 μL 1.36 M TCE solution in methanol. The reactors were mixed on a rotary shaker (30 rpm) at 25 ± 0.5℃ in an incubator. At selected intervals, 100 μL of headspace sample was withdrawn for measurement of TCE and its reaction products by gas chromatography (GC) with FID detection. The H_2 concentration in the parallel reactors was also measured, using GC-TCD. The maximum withdrawn volume from each reactor was 500 μL, which is less than 1.6% of the total

headspace volume, so no corrections for this were made.

TCE hydrodechlorination with CMC-Pd nanoparticles at varied H_2 concentrations was conducted in 120 mL glass vials sealed with PTFE septa lined caps. Typically, 60 mL of the prepared CMC-Pd nanoparticle solution and 60 mL of deionized water were filled in the reactors under magnetic stirring, which resulted in a Pd nanoparticle concentration of 10.05 mg/L. Then, these reactors were spiked with 65 μL, 130 μL, 185 μL, 260 μL, 400 μL, 650 μL and 1300 μL of pure H_2, which resulted in H/Pd atomic molar ratio of 0.5, 1, 1.4, 2, 3, 5, and 10, respectively. Then, these reactors were stored in an incubator for 24 hours at 25 ± 0.5℃ to achieve hydrogen sorption equilibrium. Then, TCE degradation was initiated by spiking 34 μL of a TCE stock solution (17.9 $g \cdot L^{-1}$) into these reactors. The resultant TCE concentration was 5 $mg \cdot L^{-1}$. At selected time intervals, 50 μL of the aqueous sample was withdrawn using a 100-μL gastight syringe. Then, the sample was transferred into a 2-mL GC vial containing 1 mL of hexane for extraction of TCE. Upon phase separation, the extract was analyzed for TCE by gas chromatography (GC) with ECD detection.

Particle Efficiencies. We define here two types of efficiencies (or selectivities) for the anaerobic ZVI-TCE-H_2O system (only significant oxidants in the system are H_2O and the contaminant). One is the efficiency of Fe(0) utilization ($\varepsilon_{Fe(0)}$), which is the molar fraction of total Fe^0 (provided by the ZVI) that reacts with TCE or H_2O (Equation 1)

$$\varepsilon_{Fe(0)} = \frac{C_{Fe^0,i} - C_{Fe^0,f}}{C_{Fe^0,i}} \quad \text{(S1)}$$

where $C_{Fe^0,i}$ and $C_{Fe^0,f}$ is the initial and final molar quantities of Fe^0.

The other type of efficiency is termed electron utilization (ε_e), which is the fraction of electron equivalents from Fe^0 that are used by reduction of TCE (to all products). To quantify ε_e requires that stoichiometries be assumed for the characteristic half reactions:

$$Fe^0 \rightarrow Fe^{2+} + 2e^- \quad \text{(S2)}$$

$$TCE + n\cdot e^- + m\cdot H^+ \rightarrow \text{products} + g\cdot Cl^- \quad \text{(S3)}$$

$$2\,H^+ + 2\,e^- \rightarrow H_2\uparrow \quad \text{(S4)}$$

The values of *n*, *m* and *g* depend on the products formed, as shown in **Table S1**. For the major products observed in this study, *n* is 4, 6, and 8 for acetylene, ethene, and ethane, respectively. The value of *n* for the overall TCE dechlorination is calculated using:

$$n = \frac{\sum_i n_i p_i}{\sum_i p_i} \quad \text{(S5)}$$

where n_i is the stoichiometry for product *i*, p_i is the molar quantity of that product.

In general, the efficiency of electron utilization (ε_e) is calculated using Equation 6:

$$\varepsilon_e = \frac{\sum_i n_i p_i}{\sum_i n_i p_i + 2M_{H_2}} \quad \text{(S6)}$$

where M_{H2} is the molar quantity of H_2 produced during the TCE dechlorination.

Both of the efficiencies reported in this study could vary with time over the

course of an experiment, so the elapsed time must be specified. In this study, the elapsed time was 8 days.

Particle Characterization. The particle crystallinity was characterized by an an X'Pert PRO XRD with a scan rate of 0.05° s^{-1}. The surface morphology and size of nZVI and S-nZVI particles were characterized using a Zeiss S-3400N SEM and a JEOL-2100F HRTEM with SEAD. XPS analyses were performed with a Kratos AXIS Ultra DLD XPS, the original binding energies were corrected according to the C1s peak at 284.8 eV, and the spectra were fit using XPS-peak4.1 software. The Fe 2p spectra were fitted assuming peaks for Fe(III), Fe(II), and Fe(0) at 711.0, 709.0, and 706.7 eV for Fe 2p3/2, and 724.8, 722.8, and 719.8 eV for Fe 2p1/2, respectively.[2, 3] In addition, the satellite peaks at 718.9 and 733.4 eV were assigned to Fe(III) and 714.6 and 729.5 eV to Fe(II).[3] The S 2p spectrum of S-nZVI was fitted with doublets (S 2p3/2 and S 2p1/2) that are separated by a spin-orbit splitting of 1.2 eV with the S 2p1/2 peak area set to half area of the S 2p3/2 peak.[4, 5] Peak assignment was based on literature reported binding energies of sulfide minerals (monosulfide (S^{2-}) at 161.5 eV, disulfide (S_2^{2-}) at 162.2 eV, and polysulfide (S_n^{2-}) at 163.1 eV).[4, 5]

The BET specific surface area of nZVI, Fe-Me, and S-nZVI were obtained by N_2 adsorption-desorption tests at 77K using a Micromeritics ASAP2020 (USA). The Fe^0 content was determined by measuring the quantity of H_2 evolved upon particle digestion in 1 M HCl and the total Fe content was concurrently obtained by measuring the dissolved Fe concentration.

Electrochemical Characterization. Experiments were performed with a three-electrode cell, using 100 mL de-oxygenated electrolyte composed of the same medium used in batch experiments (25 mM HEPES buffer, pH = 8). The electrolyte was replaced after each experiment. The cell was sparged with N_2 throughout the experiment. A glassy carbon electrode (5mm diameter) was used for the working electrode, with a Ag/AgCl (4M KCl) reference electrode and a Pt wire counter electrode, which were purchased from AIDA Hengsheng Science-Technology Development Co., ltd. (TianJin, China). Before measurement, the glassy carbon electrode was polished with nanometer Al_2O_3 powders and rinsed with deionized water. The Fe-Me, S-nZVI or nZVI (1 mg) was dispersed in a dilute Nafion solution (45 wt.%, 50 μL) by vortex mixing for 1 min. An aliquot (2 μL) of the above suspension was then coated on the clean glassy carbon electrode using a microsyringe and dried for 5 min before electrochemical analysis. All electrode modification procedure was performed in the glovebox filled with argon.

Chemical Analyses. For TCE dechlorination by all nZVI particles, TCE and reaction products in the headspace samples were analyzed using an Agilent 7890B GC with FID equipped with a GS-Q column (0.53 mm ×30 m, Agilent Technologies). The oven temperature was held at 50 ^oC for 7 min, ramped to 230 ^oC at a rate of 20 ^oC/min, and held at 230 ^oC for 10 min to separate TCE from other chlorinated and non-chlorinated degradation products. Aqueous concentrations of TCE and its dechlorination products were calculated using reported Henry's constants.

For TCE dechlorination by CMC-Pd nanoparticles, aqueous concentrations of TCE were analyzed using an Agilent 7890A GC with ECD equipped with a HP-5 column (0.32 mm ×30 m, Agilent Technologies). The injector and detector temperatures were both at 150 °C, and the oven temperature was set at 40 °C for 10 min.

H_2 was quantified on a FULI 9790 GC equipped with a packed column (3mm ×2m, Lanzhou Institute of Chemical Physics, Chinese Academy of Sciences) and a TCD detector. Argon was used as the carrier gas. The oven was isothermal at 60 °C, and the TCD temperature was set at 140 °C. Standards ranging from 0.1% to 50% hydrogen in aluminum bags were used for calibration. The dissolved Fe concentration after acid digestion was determined using a Persi TAS-990 atomic absorption spectrophotometer (AAS).

Table S1. Molar number of required electrons (n) and protons (m) for converting one mole of TCE to a specific product.

Reactant	Product	n	m
TCE	cis-DCE	2	1
	tris-DCE	2	1
	1,1-DCE	2	1
	VC	4	2
	Methane	5	3.5
	Ethene	6	3
	Acetylene	4	1
	Ethane	8	5
	Propene	6	4.5
	Propane	7.3	6.5
	Butene	6	6
	Butane	7	8
	Pentene	6	7.5
	Pentane	6.8	9.5
	Hexene	6	9
	Hexane	6.7	11

Table S2. BET surface area, Fe contents and Fe^0 contents of each particle type.

	Fe-Pd	Fe-Ni	Fe-Cu	Fe-Ag	S-nZVI	nZVI
BET surface area (m^2/g)	19	21	20	20	23	16
Fe content (%)	96.6	94.8	96.2	95.3	95.6	97.1
Initial Fe^0 content (%)	95.6	94.1	94.2	94.3	86.6	93.1

Table S3. Model-derived surface area normalized rate constants for TCE dechlorination by Fe-Me, S-nZVI and nZVI under excess TCE conditions (Me/Fe = 0.27 mol%, S/Fe = 20 mol%).

	Fe-Pd	Fe-Ni	S-nZVI
	first-order k_{SA} ($L \cdot h^{-1} \cdot m^{-2}$)	zero-order k'_{SA} ($mmol \cdot h^{-1} \cdot m^{-2}$)[b]	zero-order k'_{SA} ($mmol \cdot h^{-1} \cdot m^{-2}$)
k_1	$(8.4 \pm 0.08) \times 10^{-3}$	$5.5 \pm 0.005 \times 10^{-4}$	$1.7 \pm 0.09 \times 10^{-3}$
k_2	$8.4 \pm 0.05 \times 10^{-4}$	$2.5 \pm 0.003 \times 10^{-4}$	$4.5 \pm 0.09 \times 10^{-4}$
k_3	$5.5 \pm 0.1 \times 10^{-4}$	$3.2 \pm 0.01 \times 10^{-4}$	$3.3 \pm 0.03 \times 10^{-4}$
k_4	$1.9 \pm 0.01 \times 10^{-3}$	$5 \pm 0.05 \times 10^{-4}$	$2.3 \pm 0.1 \times 10^{-4}$
k_{TCE}[a]	$9.9 \pm 0.4 \times 10^{-3}$	$1.1 \pm 0.02 \times 10^{-3}$	$1.7 \pm 0.09 \times 10^{-3}$
	Fe-Ag	Fe-Cu	nZVI
	zero-order k'_{SA} ($mmol \cdot h^{-1} \cdot m^{-2}$)	zero-order k'_{SA} ($mmol \cdot h^{-1} \cdot m^{-2}$)	zero-order k'_{SA} ($mmol \cdot h^{-1} \cdot m^{-2}$)
k_{TCE}[a]	$7.2 \pm 0.07 \times 10^{-5}$	$1.3 \pm 0.02 \times 10^{-4}$	$8.8 \pm 0.2 \times 10^{-6}$

[a] $k_{TCE} = k_1 + k_2 + k_3$ for Fe-Me, $k_{TCE} = k_1$ for S-nZVI. [b] k' = zero-order rate constant = initial rate.

Table S4. Estimated zero-order rate constants for TCE dechlorination by Fe-Pd (0.27 mol%) and S-nZVI (0.27 mol%) under excess TCE conditions.

	Fe-Pd	S-nZVI
	zero-order k'_{SA} ($mmol \cdot h^{-1} \cdot m^{-2}$)	zero-order k'_{SA} ($mmol \cdot h^{-1} \cdot m^{-2}$)
k_{TCE}	$6.0 \pm 0.06 \times 10^{-2}$	$1.9 \pm 0.03 \times 10^{-4}$

Table S5. Corrosion currents of Fe-Me, S-nZVI, and nZVI.

	Fe-Pd	Fe-Ni	Fe-Cu	Fe-Ag	S-nZVI	nZVI
Corrosion current (A)	-2.3×10^{-6}	-1.7×10^{-6}	-9.9×10^{-7}	-8.0×10^{-7}	-1.0×10^{-6}	-6.1×10^{-7}

Table S6. Values of the standard Gibbs energy of adsorption of hydrogen on each metal surface.

Metals	Pd	Ni	Cu	Ag
ΔG_H^∞ (eV)[a]	-0.14	-0.27	0.19	0.51

[a] The values of ΔG_H^∞ were obtained from Nørskov et al.[6]

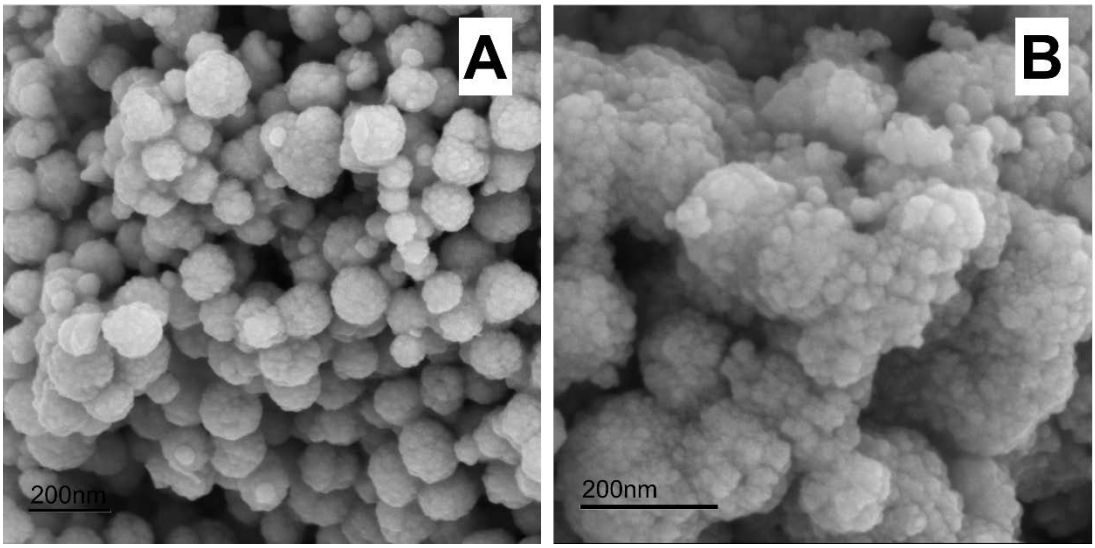

Figure S1. Scanning electron microscopy (SEM) images of nZVI (A) and S-nZVI (B).

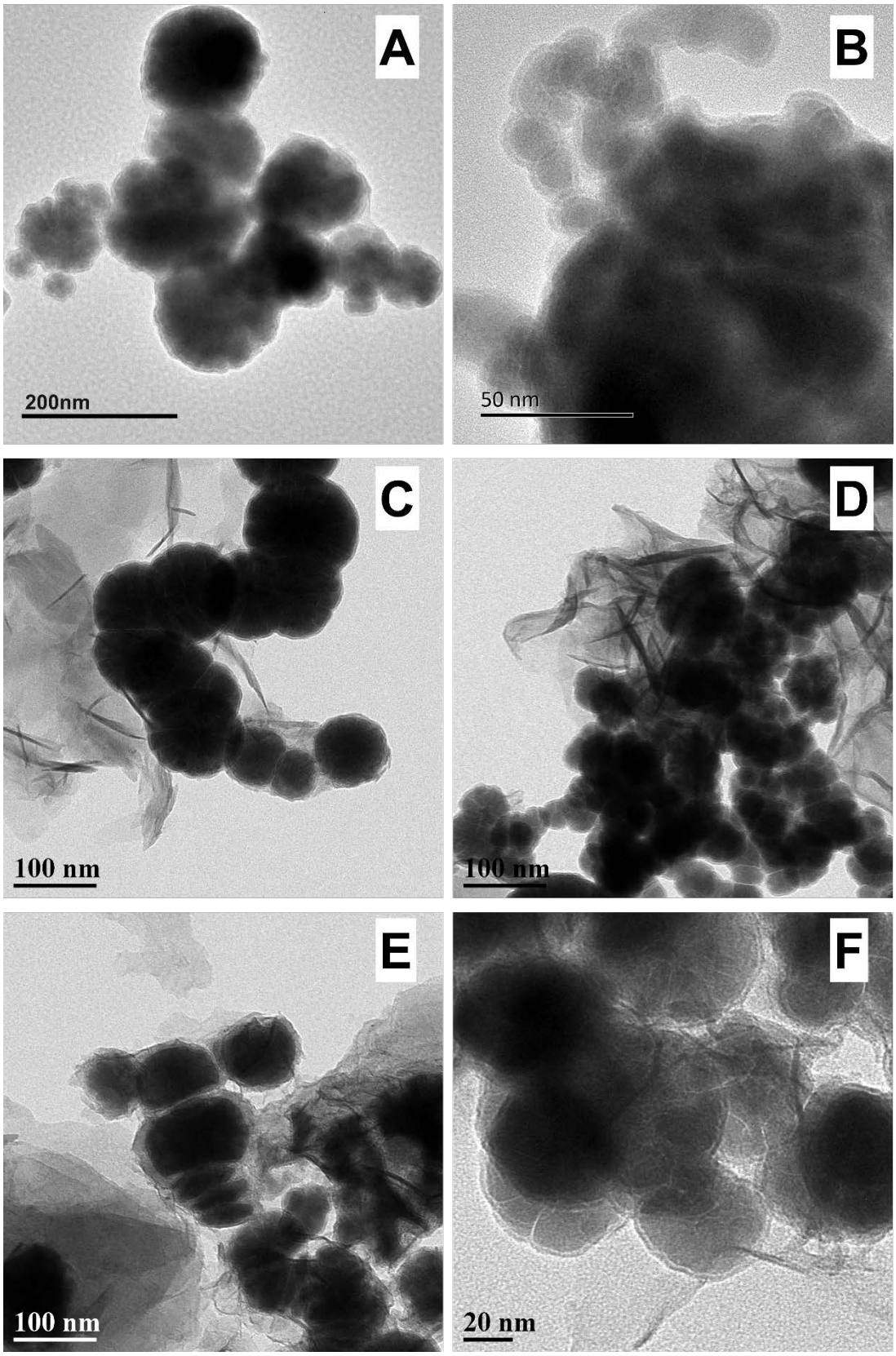

Figure S2. Transmission electron microscopy (TEM) images of nZVI (A), S-nZVI (B), Fe-Pd (C), Fe-Ni (D), Fe-Cu (E) and Fe-Ag (F) (S/Fe = 20 mol%, and Me/Fe = 0.27 mol%).

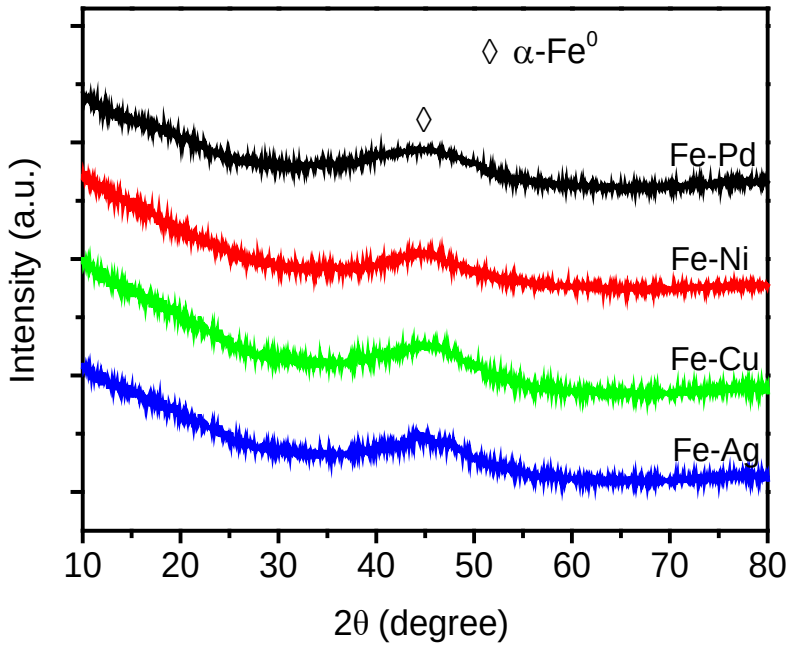

Figure S3. XRD patterns of Fe-Me particles (Me/Fe = 0.27 mol%).

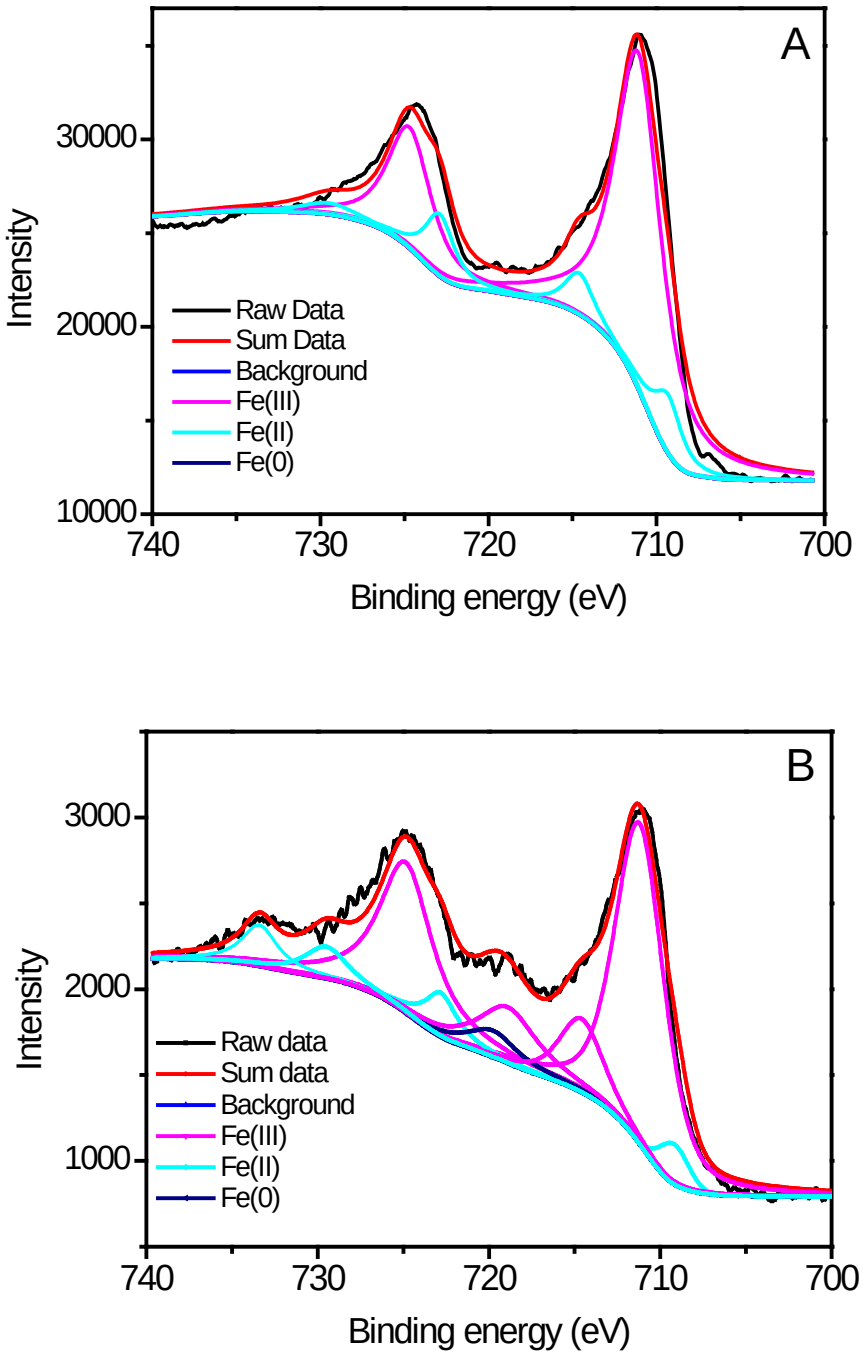

Figure S4. Fe 2p XPS spectra of nZVI (A) and S-nZVI (S/Fe = 20 mol%) (B).

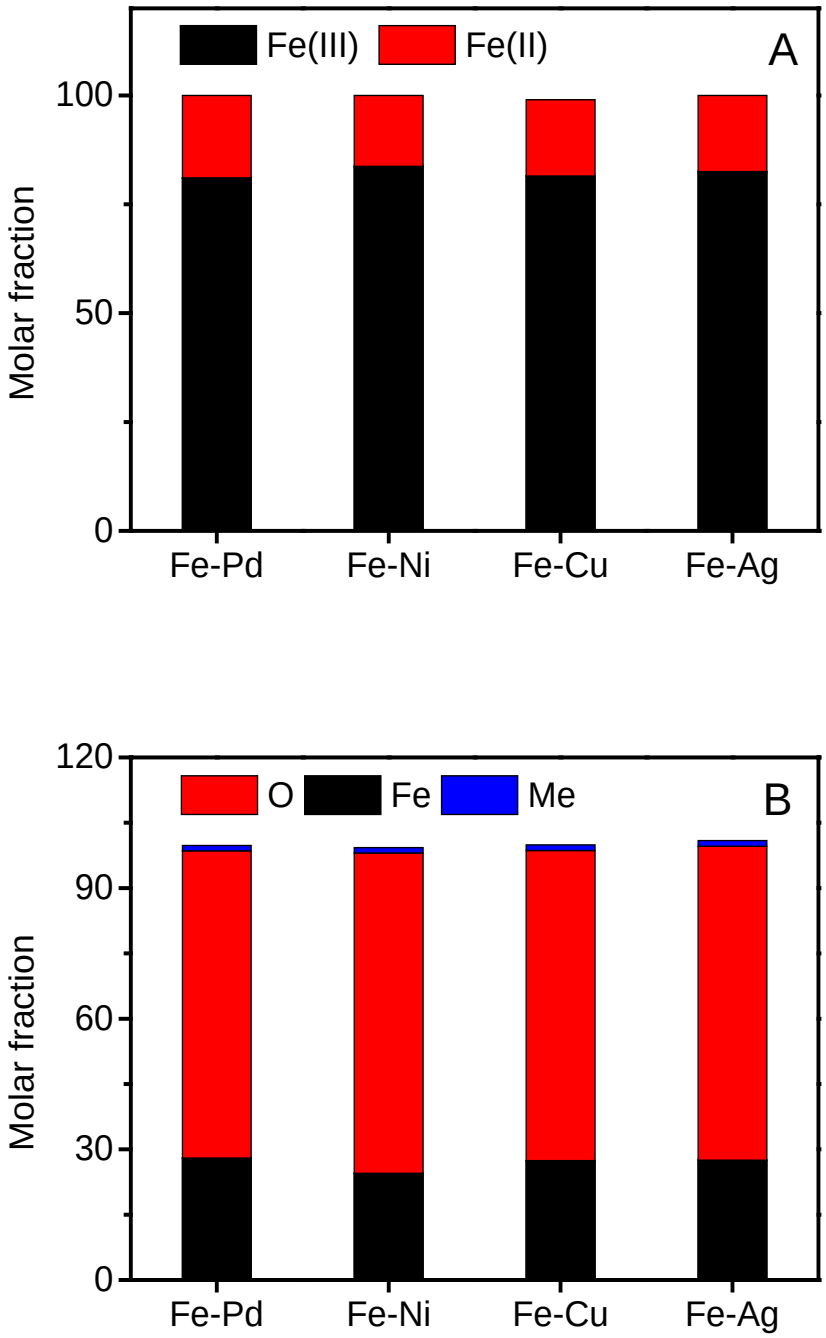

Figure S5. Molar fraction of Fe(II) and Fe(III) in each Fe-Me particle derived from fitting of XPS Fe 2p spectra (A) and molar fraction of Fe, O, and Me content in each Fe-Me particle (B) (Me/Fe = 0.27 mol%).

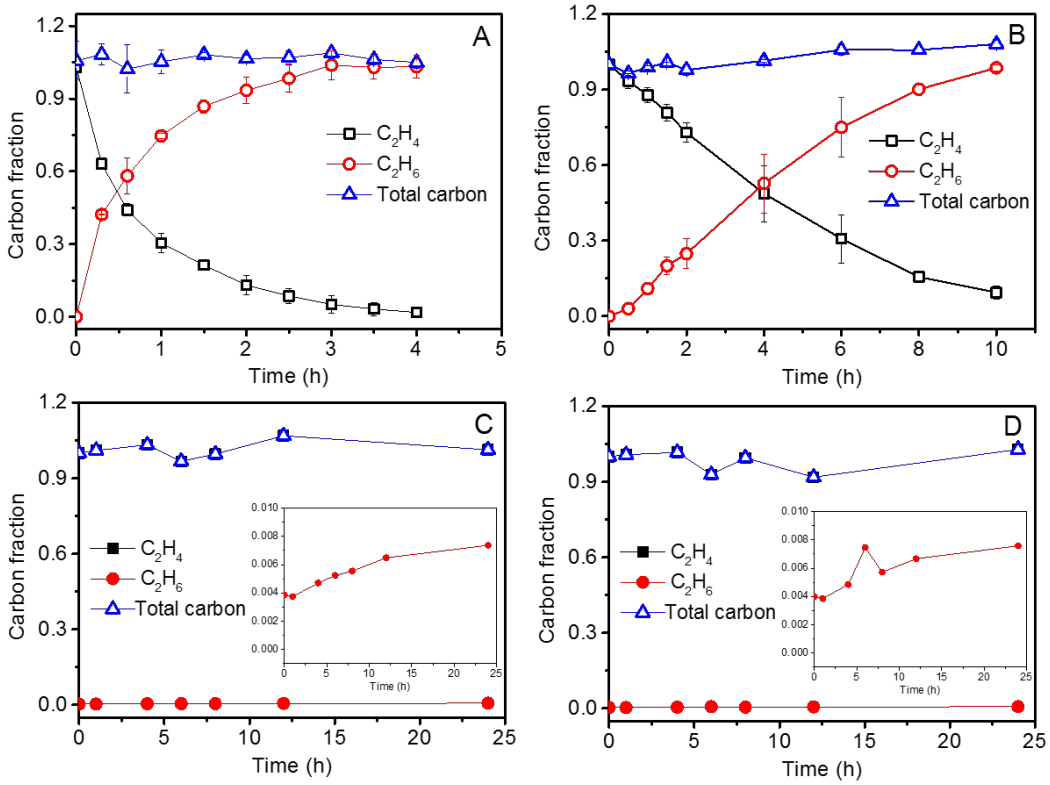

Figure S6. Ethene reduction and formation of reaction products by Fe-Pd (A), Fe-Ni (B), Fe-Cu (C) and Fe-Ag (D).

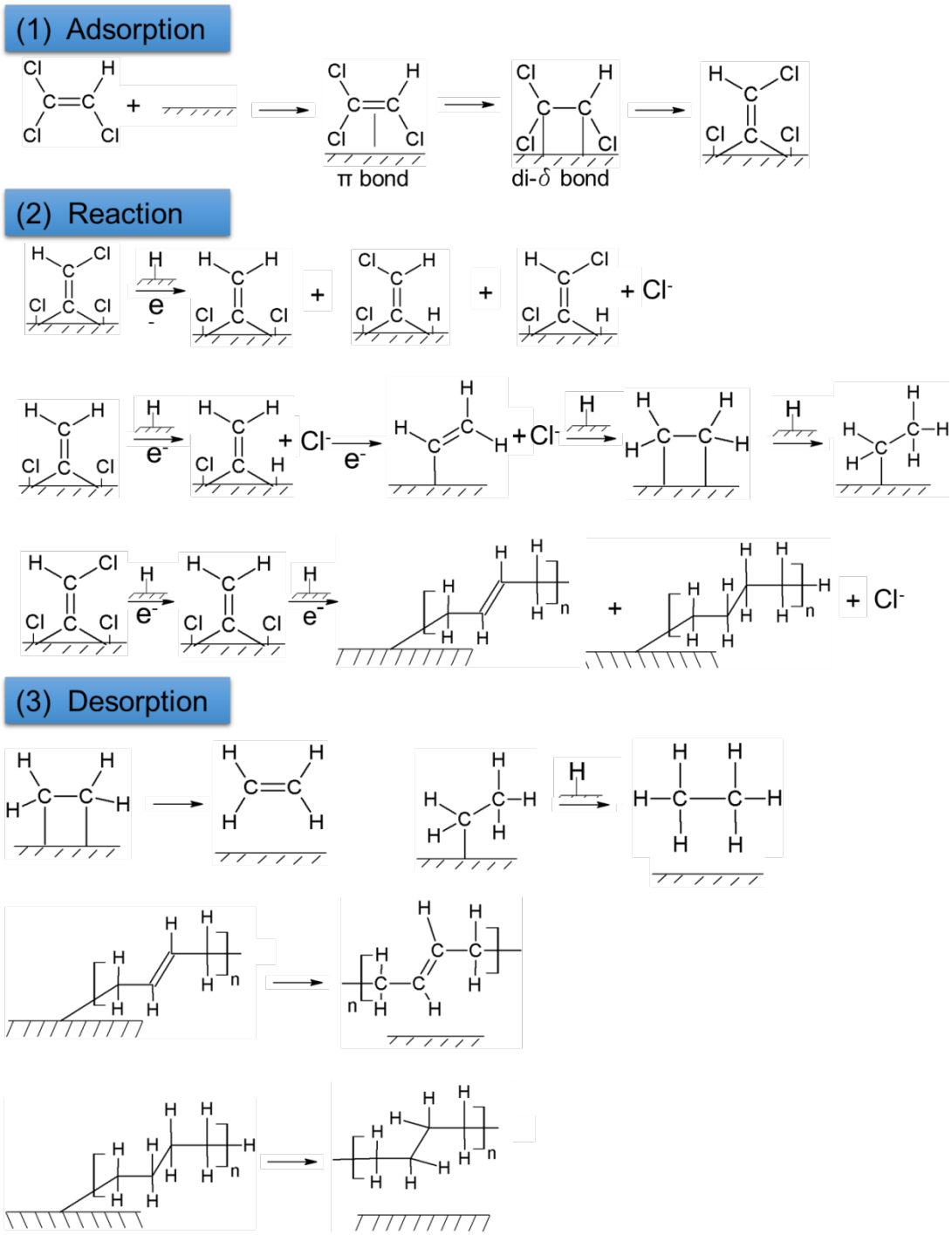

Figure S7. The proposed TCE dechlorination process on the surface of Fe-Me bimetallic particles (Fe-Pd as an example) based on results from this study and previous researches.[7-13]

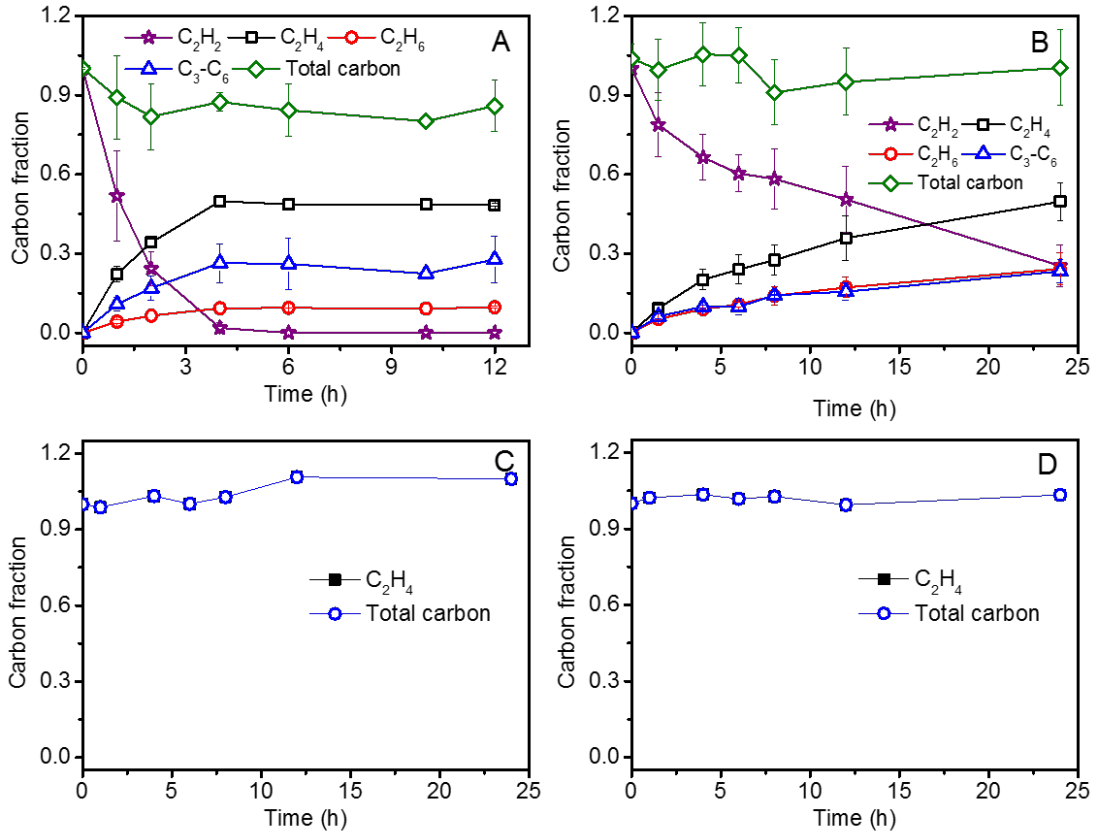

Figure S8. Acetylene reduction and formation of reaction products by S-nZVI (A) and nZVI (B) and ethene reduction and formation of reaction products by S-nZVI (C) and nZVI (D).

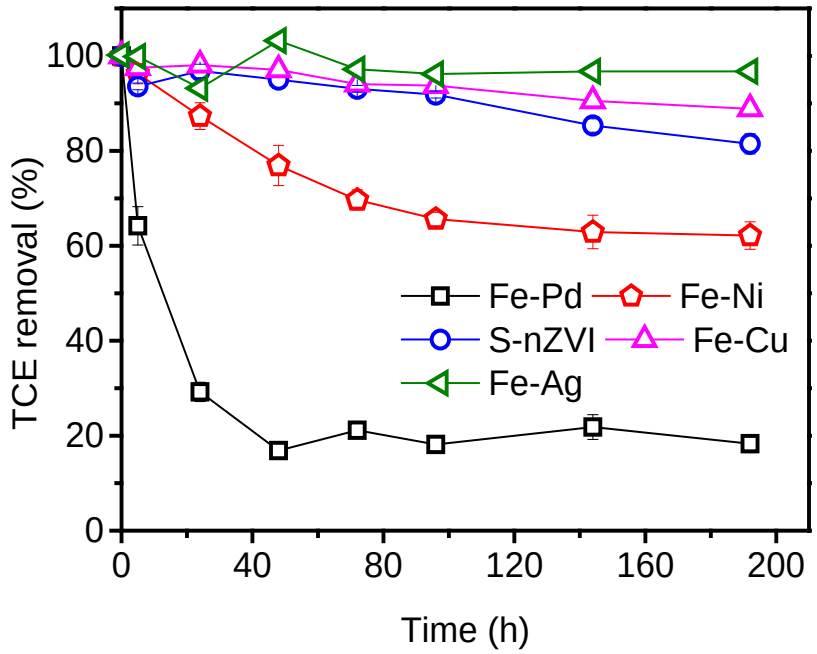

Figure S9. Comparison of TCE dechlorination by Fe-Me and S-nZVI at same Me/Fe and S/Fe molar ratio of 0.27 mol%.

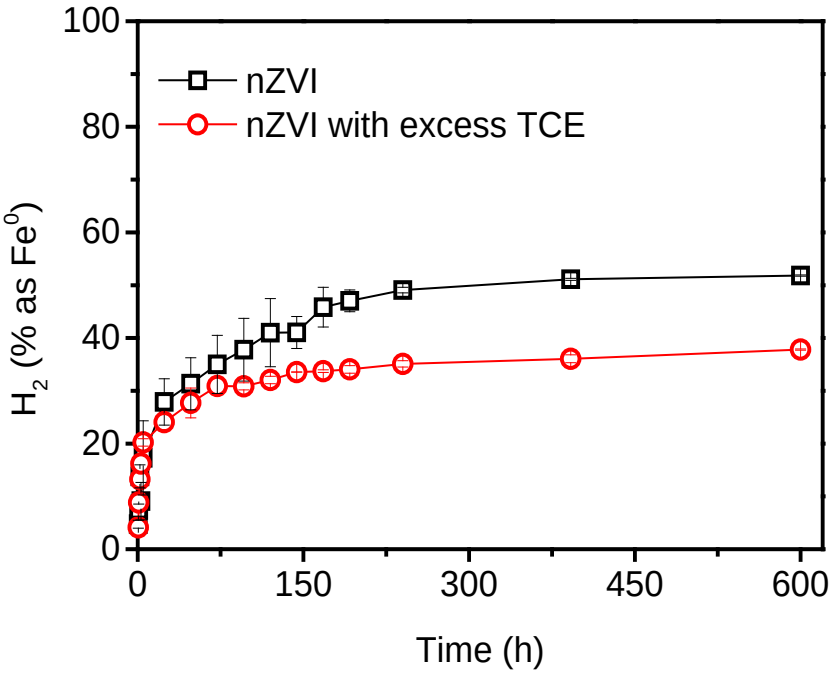

Figure S10. H_2 evolution of nZVI with and without excess TCE in an extended period of time (up to 25 days).

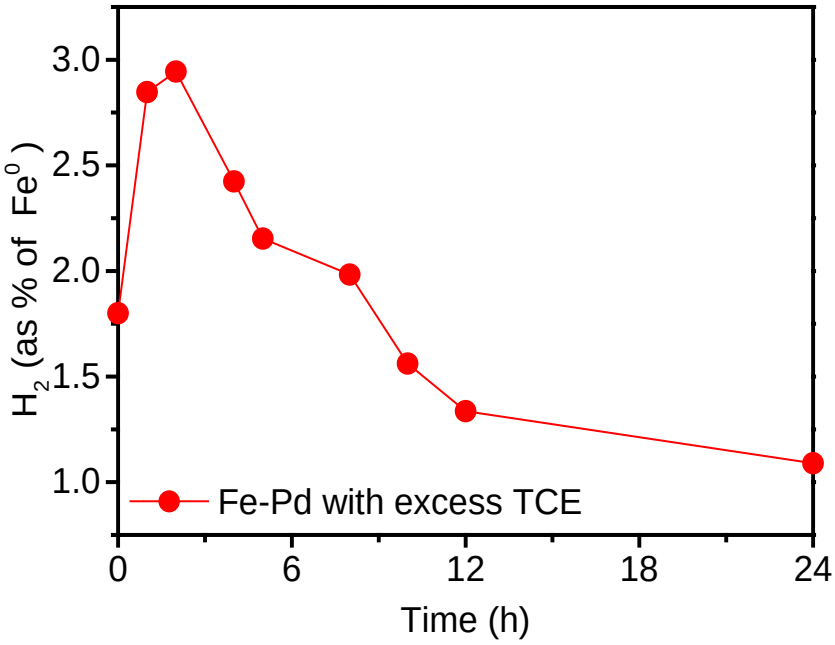

Figure S11. A closer look of H_2 evolution during TCE dechlorination by Fe-Pd.

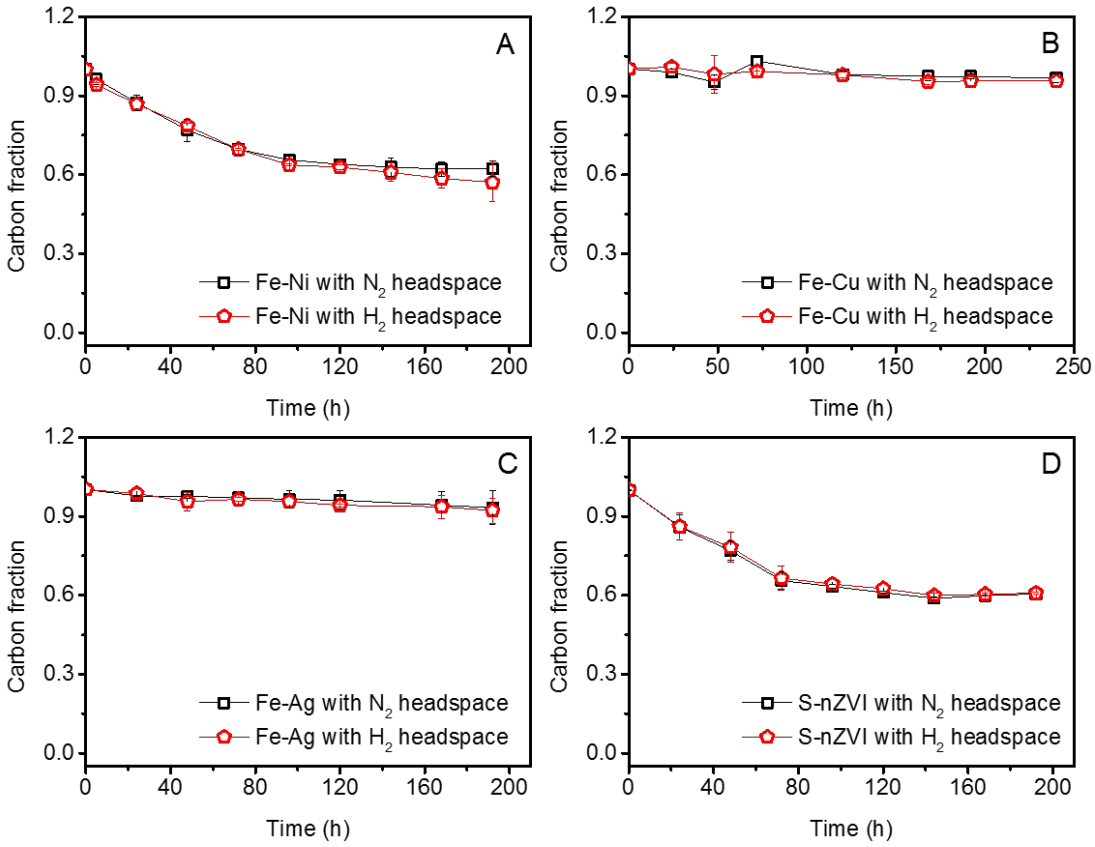

Figure S12. TCE dechlorination in batch reactors with Ar and H2 headspaces by Fe-Ni (A), Fe-Cu (B), Fe-Ag (C), and S-nZVI (D) under excess TCE conditions (Me/Fe = 0.27 mol%, S/Fe = 20 mol%). All experiments at pH 8 buffered by 25 mM HEPES and under anoxic conditions.,

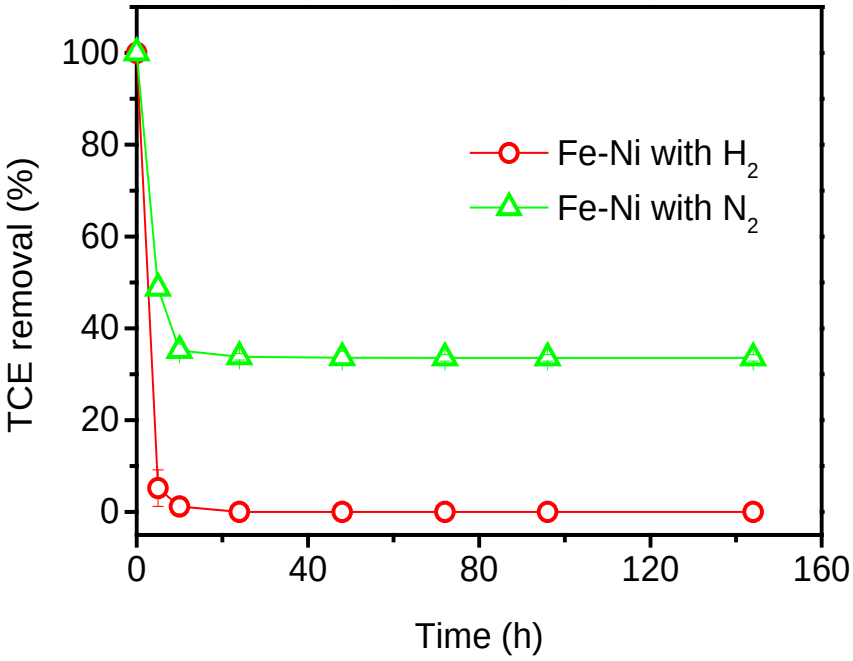

Figure S13. TCE dechlorination in batch reactors with Ar and H_2 headspaces by Fe-Ni under excess TCE conditions (Ni/Fe = 20 mol%).

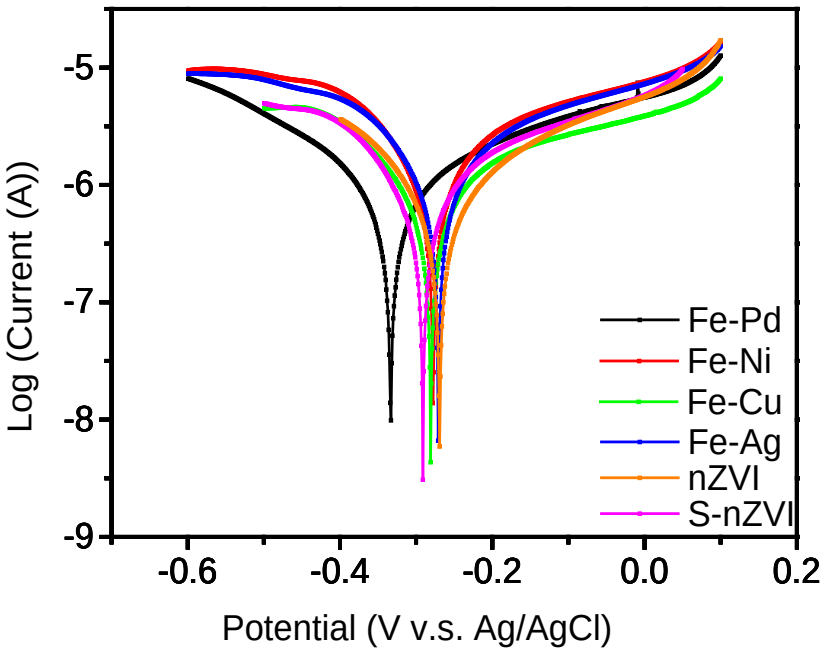

Figure S14. Tafel scans of working electrode made from Fe-Me, S-nZVI and nZVI particles.

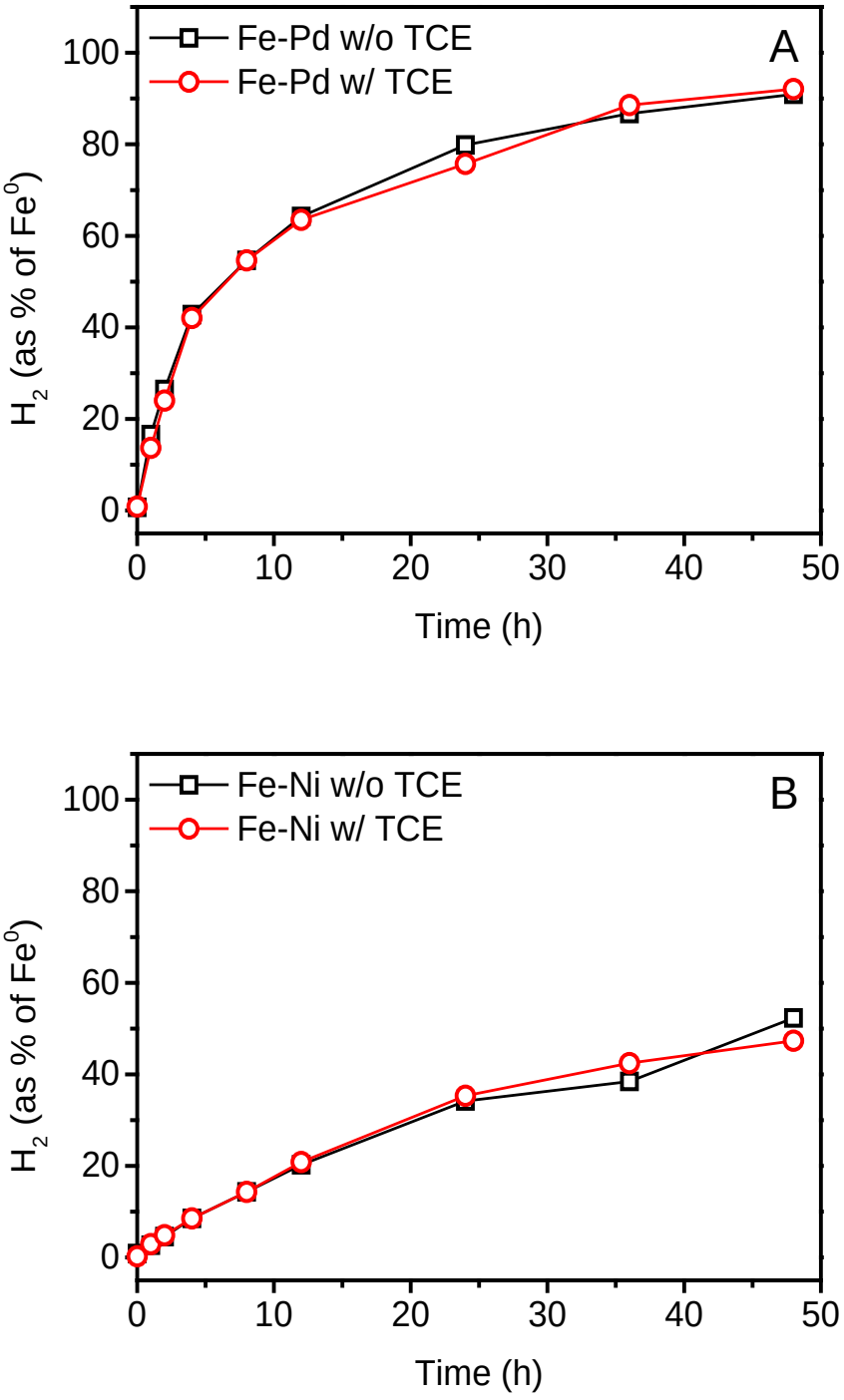

Figure S15. H_2 evolution of Fe-Pd (A) and Fe-Ni (B) with and without TCE under excess iron conditions (Fe: 1g L^{-1}, TCE: 10 mg L^{-1}). All experiments at pH 8 buffered by 25 mM HEPES and under anoxic conditions. The almost same H_2 production for Fe-Pd and Fe-Ni in the absence and presence of limited TCE suggests that TCE did not affect HER under excess iron conditions.

References

1. Liu, Y. Q.; Majetich, S. A.; Tilton, R. D.; Sholl, D. S.; Lowry, G. V., TCE dechlorination rates, pathways, and efficiency of nanoscale iron particles with different properties. *Environ. Sci. Technol.* 2005, *39*, (5), 1338-1345.
2. Xu, H.; Sun, Y.; Li, J.; Li, F.; Guan, X., Aging of Zerovalent Iron in Synthetic Groundwater: X-ray Photoelectron Spectroscopy Depth Profiling Characterization and Depassivation with Uniform Magnetic Field. *Environ. Sci. Technol.* 2016, *50*, (15), 8214-22.
3. Yamashita, T.; Hayes, P., Analysis of XPS spectra of Fe2+ and Fe3+ ions in oxide materials. *Appl. Surf. Sci.* 2008, *254*, (8), 2441-2449.
4. Lan, Y.; Butler, E. C., Iron-Sulfide-Associated Products Formed during Reductive Dechlorination of Carbon Tetrachloride. *Environ. Sci. Technol.* 2016, *50*, (11), 5489-5497.
5. Smart, R. S.; Skinner, W. M.; Gerson, A. R., XPS of sulphide mineral surfaces: Metal-deficient, polysulphides, defects and elemental sulphur. *Surf. Interface Anal.* 1999, *28*, (1), 101-105.
6. Nørskov, J. K.; Bligaard, T.; Logadottir, A.; Kitchin, J. R.; Chen, J. G.; Pandelov, S.; Stimming, U., Trends in the Exchange Current for Hydrogen Evolution. *J. Electrochem. Soc.* 2005, *152*, (3), J23.
7. Chaplin, B. P.; Reinhard, M.; Schneider, W. F.; Schuth, C.; Shapley, J. R.; Strathmann, T. J.; Werth, C. J., Critical review of Pd-based catalytic treatment of priority contaminants in water. *Environ. Sci. Technol* 2012, *46*, (7), 3655-70.
8. Butler, E. C.; Hayes, K. F., Factors influencing rates and products in the transformation of trichloroethylene by iron sulfide and iron metal. *Environ. Sci. Technol.* 2001, 35, (19), 3884-3891.
9. Arnold, W. A.; Roberts, A. L., Pathways and Kinetics of Chlorinated Ethylene and Chlorinated Acetylene Reaction with Fe(0) Particles. *Environ. Sci. Technol.* 2000, 34, (9), 1794-1805.
10. Hansen, E. W.; Neurock, M., First-Principles-Based Monte Carlo Simulation of Ethylene Hydrogenation Kinetics on Pd. *J. Catal.* 2000, 196, (2), 241-252.
11. Marsh, A. L.; Somorjai, G. A., Structure, reactivity, and mobility of carbonaceous overlayers during olefin hydrogenation on platinum and rhodium single crystal surfaces. *Top. Catal.* 2005, 34, (1), 121-128.
12. Heck, K. N.; Janesko, B. G.; Scuseria, G. E.; Halas, N. J.; Wong, M. S., Observing Metal-Catalyzed Chemical Reactions in Situ Using Surface-Enhanced Raman Spectroscopy on Pd-Au Nanoshells. *J. Am. Chem. Soc.* 2008, 130, (49), 16592-16600.
13. Li, S.; Fang, Y.-L.; Romanczuk, C. D.; Jin, Z.; Li, T.; Wong, M. S., Establishing the trichloroethene dechlorination rates of palladium-based catalysts and iron-based reductants. *Appl. Catal. B: Environ.* 2012, 125, 95-102.